

Time-Resolved Studies of Fluorescence Quenching in Supercritical Carbon Dioxide: System Dependence in the Enhancement of Bimolecular Reaction Rates at Near-Critical Densities

Christopher E. Bunker and Ya-Ping Sun*

Department of Chemistry, Howard L. Hunter Chemistry Laboratory, Clemson University, Clemson, South Carolina 29634-1905

James R. Gord*

Aero Propulsion and Power Directorate, Wright Laboratory, Wright-Patterson Air Force Base, Ohio 45433-7103

Received: August 22, 1997[Ⓞ]

The quenching of anthracene, perylene, 9-cyanoanthracene (9CA), and 9,10-diphenylanthracene (DPA) excited singlet states by carbon tetrabromide (CBr₄) in supercritical CO₂ has been studied systematically by use of the time-resolved fluorescence method. For 9CA–CBr₄ and DPA–CBr₄, there is enhanced fluorescence quenching at near-critical CO₂ densities. On the other hand, the CO₂ density dependence of fluorescence quenching in the anthracene–CBr₄ and perylene–CBr₄ systems follows the prediction of the hydrodynamic Smoluchowski equation for diffusion-controlled reactions. The results show, for the first time, that the enhancement in bimolecular fluorescence quenching reactions due to effects of local quencher concentration augmentation in supercritical CO₂ is in fact system dependent.

Introduction

Supercritical fluids are unique solvent systems that have received much attention.^{1–3} The most important properties of a supercritical fluid are the low densities, which are between those of a gas and a liquid and are easily tunable with changes in pressure isothermally, and the clustering effects. Solute–solvent clustering and solute–solute clustering in supercritical fluids have been studied extensively, and their effects on unimolecular and bimolecular chemical processes have been evaluated. While solute–solvent clustering in which the local density of solvent molecules surrounding a solute molecule is higher than the bulk density has been demonstrated by using spectroscopic and other techniques for a series of molecular probes,^{4–16} the existence and properties of the solute–solute clustering in supercritical fluids are still subject to debate.^{17–23} The concept of solute–solute clustering was proposed initially on the basis of observations of entrainer effects in supercritical fluid extraction, namely, that solubilities in a supercritical fluid are significantly increased with the presence of a small fraction of liquid cosolvent.²⁴ Although a rigorous definition of solute–solute clustering in supercritical fluids is not available, the clustering may be understood in terms of a locally higher solute concentration than the bulk concentration as a result of the microscopically inhomogeneous nature of the fluid at near-critical densities.²³ While experimental observations that may be explained in terms of local solute concentration augmentation effects have been reported, other evidence that is against the existence of such effects has also been presented.^{18–23} The proposed clustering effects appear to be system dependent. We have recently used the quenching of the 9,10-bis(phenylethynyl)-anthracene (BPEA) excited singlet state by carbon tetrabromide (CBr₄), which is known to be a simple bimolecular reaction, in the study of solute–solute clustering effects in supercritical CO₂.^{23a} The apparent quenching rate constants, which were obtained from time-resolved fluorescence measurements, are dependent on the CO₂ density following a different pattern from

what is predicted by the classical hydrodynamic model for diffusion-controlled reactions. The enhanced quenching of the BPEA excited singlet state by CBr₄ at near-critical CO₂ densities may be attributed to a higher local CBr₄ concentration in the vicinity of an excited BPEA molecule.^{23a} However, in order to understand the results in a broader context, excited-state quenching reactions in other arene–CBr₄ systems are examined systematically. Here we report a study of anthracene, 9-cyanoanthracene (9CA), 9,10-diphenylanthracene (DPA), and perylene fluorescence lifetime quenching by CBr₄ in supercritical CO₂ at a series of densities. The 9CA–CBr₄ and DPA–CBr₄ systems are similar to BPEA–CBr₄, exhibiting enhanced fluorescence quenching at near-critical CO₂ densities. On the other hand, the CO₂ density dependence of fluorescence quenching in the anthracene–CBr₄ and perylene–CBr₄ systems follows the prediction of the hydrodynamic Smoluchowski equation for diffusion-controlled reactions. The results show, for the first time, that the enhancement in bimolecular fluorescence quenching reactions due to effects of local quencher concentration augmentation in supercritical CO₂ is in fact system dependent.

Experimental Section

Materials. Anthracene (99%), 9-cyanoanthracene (97%), 9,10-diphenylanthracene (97%), perylene (99+ %), and carbon tetrabromide (99%) were obtained from Aldrich and used without further purification. Hexane and cyclohexane (spectrophotometry grade) were obtained from Burdick & Jackson and used as received. CO₂ (99.9999%) was obtained from Air Products. The oxygen content was checked by comparing fluorescence quantum yields of pyrene before and after a rigorous deoxygenation procedure in which the CO₂ was repeatedly passed through oxygen traps obtained from Alltech Associates. Because the results indicated no oxygen quenching, the CO₂ was used without further purification.

Measurements. Absorption spectra were recorded on a computer-controlled Shimadzu UVPC-2101 spectrophotometer. Steady-state fluorescence spectra were obtained on a Spex

[Ⓞ] Abstract published in *Advance ACS Abstracts*, November 15, 1997.

Fluorolog-2 photon-counting emission spectrometer equipped with a 450 W xenon source, a Spex 1681 monochromator for excitation and a Spex 350S monochromator for emission, and a detector consisting of a Hamamatsu R928 photomultiplier tube operated at -950 V. Excitation and emission slits were 0.25 mm (1 nm resolution) and 1.25 mm (5 nm resolution), respectively. Fresh solutions were used in all measurements to minimize the effect of possible photochemical reactions. All fluorescence spectra were corrected for nonlinear instrumental response of the spectrometer using predetermined correction factors.

Fluorescence decays were measured by using the time-correlated single photon counting (TCSPC) method. For measurements in liquid solvents, the TCSPC setup includes a nitrogen flash lamp obtained from Edinburgh Instruments as the excitation source. The flash lamp was operated at 50 kHz, and the wavelength of 317 nm was isolated using a band-pass filter with 10 nm fwhm. Fluorescence decays were monitored through a 545 nm color glass sharp-cut filter. The detector consists of a Philips X2020 photomultiplier tube in a thermoelectrically cooled housing obtained from the Products for Research, Co. The photomultiplier tube was operated at -2 kV using an EG&G 556 high-voltage power supply. The detector electronics from EG&G Ortec include two 9307 discriminators, a 457 biased time-to-amplitude converter, and a 916A multichannel analyzer. The instrument response function of the setup has a fwhm of ~ 2.0 ns. The TCSPC setup for the measurement of fluorescence decays in supercritical CO_2 includes a Spectra-Physics 3690 Tsunami mode-locked Ti:sapphire laser as the excitation source. The laser was configured to produce an 82 MHz train of pulses at 720 – 775 nm with a nominal pulse width of less than 2 ps. The repetition rate of the pulse train was reduced to 4 MHz using a Spectra-Physics 3980 pulse selector. The laser output was frequency-doubled using a phase matched LBO crystal obtained from CSK Optonics. Fluorescence decays were monitored through an American Holographic DB-10S double subtractive monochromator. The detector consists of a Hamamatsu R3809U-01 microchannel plate photomultiplier tube (MCP-PMT) in a Hamamatsu C2773 thermoelectrically cooled housing. The MCP-PMT tube was biased at -3 kV using a Stanford Research Systems PS350 power supply. The detector electronics consists of two EG&G Ortec 9307 discriminators, a Tennelec TC-864 time-to-amplitude converter/biased amplifier, and a Tennelec PCA-Multiport-E multichannel analyzer. The instrument response function of the setup has a fwhm of ~ 60 ps. Fluorescence lifetimes were determined from observed decay curves and instrument response functions by use of the Marquardt nonlinear least-squares method.²⁵

The high-pressure setup for spectroscopic studies in supercritical CO_2 is similar to the one reported previously.²³ The system pressure was generated by a Teflon-packed syringe pump (High Pressure Equipment Co., 87-6-5) and monitored by a precision pressure gauge (Dresser Industries, Heise-901A). The calibrated accuracy of the pressure gauge is ± 1 psia at 1100 psia. The system temperature was controlled and monitored by an RTD temperature controller (Omega, 4200A) coupled with a pair of cartridge heaters (Gauger, 150W) inserted into the optical cell body. Absorption and fluorescence measurements were carried out using a cubic shaped high-pressure optical cell made from stainless steel. The cell chamber (calibrated volume 1.87 mL) consists of four channels which open at the four side walls of the cell. Three of the channels are for accommodating optical windows and the fourth one is for cell cleaning. The three quartz windows (12.7 mm diameter and 5 mm thick) are

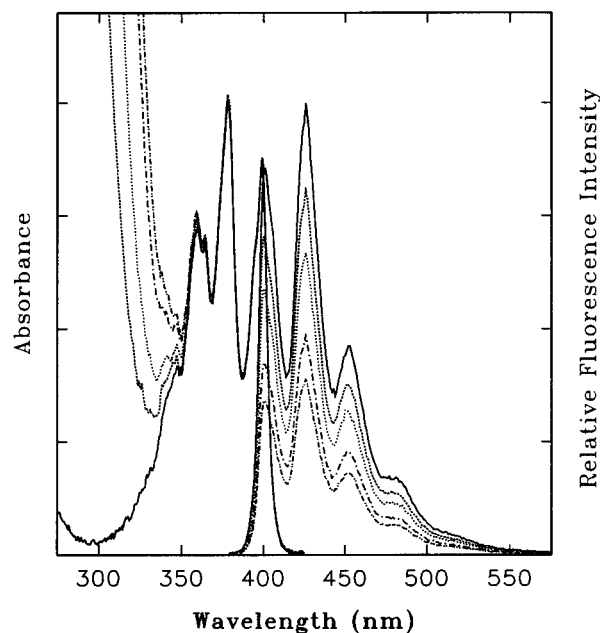


Figure 1. Absorption and fluorescence spectra of 9CA in room-temperature hexane at CBr_4 concentrations of 0 (—), 2.4×10^{-3} (---), 4.5×10^{-3} (···), 9.6×10^{-3} (-.-), and 1.26×10^{-2} M (-.-.-).

sealed using Teflon O-rings. The optical paths of the cell for absorption (180°) and fluorescence (90°) measurements are 30.5 and 7.5 mm (both calibrated), respectively.

In the preparation of samples for fluorescence measurements in supercritical CO_2 , hexane solutions of the fluorophores were added to the high-pressure optical cell. The cell was purged with a slow stream of nitrogen gas to remove the solvent hexane, followed by the addition of a small quantity of CBr_4 solid. A procedure of repeatedly filling and discharging with low-pressure CO_2 gas (< 100 psia) was used to eliminate trace amounts of oxygen trapped in the optical cell chamber. The cell was then sealed and thermostated at the desired temperature before CO_2 was introduced. The CBr_4 concentrations were determined spectroscopically using a calibration curve based on absorption in the wavelength region of 250 – 320 nm.

Viscosity values under our experimental conditions were obtained through interpolation from the experimental results reported in the literature²⁶ by using the empirical equation due to Jossi, Stiel, and Thodos.²⁷

Results

In Solution. Absorption and fluorescence spectra of anthracene, 9CA, DPA, and perylene were measured in room-temperature (22°C) hexane at different CBr_4 concentrations. The results for 9CA are shown in Figure 1. The absorption spectra are CBr_4 concentration independent, with the changes in the blue region (< 350 nm) due to CBr_4 absorptions. The fluorescence spectra are independent of excitation wavelength. As shown in Figure 1 for 9CA, the observed fluorescence spectral profiles remain essentially the same while the fluorescence intensities decrease systematically with increasing CBr_4 concentrations. The intensity quenching ($R = \Phi_F^\circ/\Phi_F$) follows the linear Stern–Volmer relationship

$$R = 1 + k_q \tau_F^\circ [\text{CBr}_4] \quad (1)$$

where k_q is the quenching rate constant and τ_F° is the unquenched fluorescence lifetime. A Stern–Volmer plot for 9CA that includes results obtained at different excitation wavelengths is shown in Figure 2. The quenching is apparently

TABLE 1: Fluorescence Quenching Results of the Arene-CBr₄ Systems

	hexane			cyclohexane			supercritical CO ₂					
	τ_F , ns	$k_q \times 10^{10}$, M ⁻¹ s ⁻¹	f^a	τ_F , ns	$k_q \times 10^{10}$, M ⁻¹ s ⁻¹	f^a	$k_q \times 10^{10}$, M ⁻¹ s ⁻¹ for $\rho_r =$					$f_{1.8}^c$
							1.0	1.2	1.4	1.6	1.8	
anthracene	5.36	3.0	1.4	5.41	1.25 ^b	1.8	4.0	3.3	2.8	2.3	2.0	0.21
perylene	5.29	2.1	1.0				5.1	4.1	3.4	2.8	2.4	0.26
9CA	14.2	0.76	0.36				2.2	1.6	1.2	0.9	0.79	0.088
DPA	7.75	2.0	0.97				5.6	4.2	3.3	2.6	2.1	0.25

^a $f = k_q/k_{diff}$. ^b The literature value is 1.3×10^{10} M⁻¹ s⁻¹ (ref 28). ^c f at $\rho_r = 1.8$.

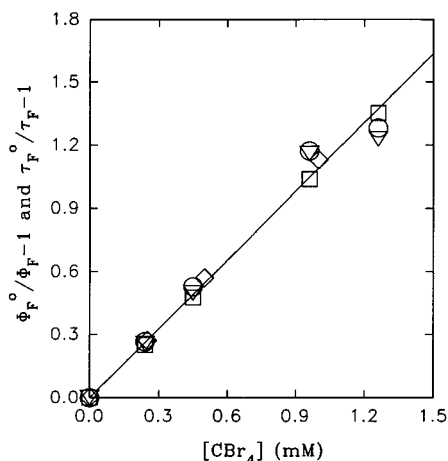


Figure 2. Stern–Volmer plots for 9CA fluorescence lifetime quenching τ_F°/τ_F (\diamond) and quantum yield quenching Φ_F°/Φ_F at different excitation wavelengths (358 nm, \circ ; 369 nm, \square ; 394 nm, ∇) by CBr₄ in room-temperature hexane. The line is from a global linear least-squares regression with a slope of 109 M⁻¹.

excitation wavelength independent. A linear least-squares regression yields a Stern–Volmer constant $k_q\tau_F^\circ$ of 108 M⁻¹.

Fluorescence decays were also measured in room-temperature hexane as a function of CBr₄ concentration. The decays can be well described by convolution of the corresponding instrumental response functions with a monoexponential equation. For 9CA, results of the fluorescence lifetime quenching by CBr₄ are in excellent agreement with those from the fluorescence intensity quenching (Figure 2). The lifetime quenching also follows the linear Stern–Volmer relationship ($R = \tau_F^\circ/\tau_F$, eq 1). A linear least-squares regression that includes both fluorescence intensity and lifetime quenching results of 9CA–CBr₄ yields $k_q\tau_F^\circ$ of 109 M⁻¹. With the known 9CA fluorescence lifetime τ_F° of 14.2 ns, the quenching rate constant k_q is 7.6×10^9 M⁻¹ s⁻¹ in hexane (Table 1).

The quenching results for anthracene–CBr₄, DPA–CBr₄, and perylene–CBr₄ in room-temperature hexane are similar to those of 9CA–CBr₄. The quenching rate constants obtained from Stern–Volmer plots are summarized in Table 1. For anthracene, the quenching of fluorescence by CBr₄ was also studied in a somewhat more viscous solvent cyclohexane at room temperature. While the fluorescence intensity and lifetime quenchings of anthracene by CBr₄ in cyclohexane also follow the linear Stern–Volmer relationship (eq 1, Figure 3), the quenching rate constant k_q in cyclohexane (1.25×10^{10} M⁻¹ s⁻¹) is significantly smaller than that in hexane (3.0×10^{10} M⁻¹ s⁻¹).

In Supercritical CO₂. Fluorescence decays of anthracene, 9CA, DPA, and perylene were measured in supercritical CO₂ as a function of reduced density (defined as density/the critical density) at 35 °C and at different quencher CBr₄ concentrations. Shown in Figure 4 are representative results for 9CA in supercritical CO₂ with and without the quencher CBr₄. The decay curves can all be well described using a monoexponential function. There is no evidence for any deviations from single-

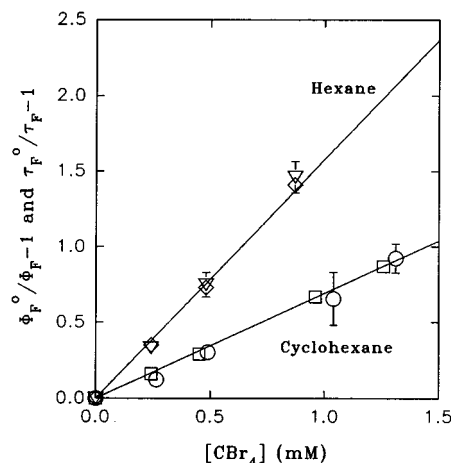


Figure 3. Stern–Volmer plots for quenchings of anthracene fluorescence lifetime τ_F°/τ_F (\diamond in hexane and \square in cyclohexane) and quantum yield Φ_F°/Φ_F (∇ in hexane and \circ in cyclohexane) by CBr₄ at room temperature. The lines are from linear least-squares regressions with slopes of 161 and 68 M⁻¹ in hexane and cyclohexane, respectively.

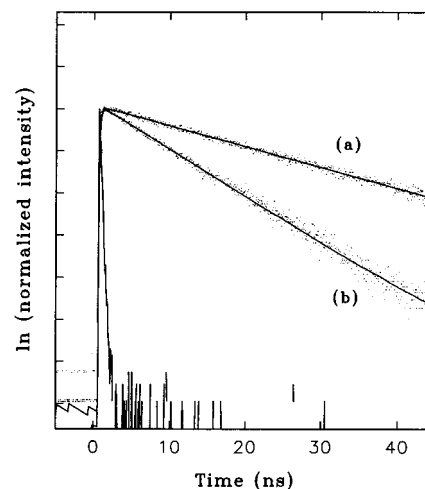


Figure 4. Fluorescence decays of 9CA in CO₂ at a reduced density of 1.0 at 35 °C and CBr₄ concentrations of (a) 0 ($\tau_F = 19.4$ ns and $\chi^2 = 1.13$) and (b) 2.9×10^{-3} M ($\tau_F = 9.0$ ns and $\chi^2 = 1.07$). The instrument response function obtained under the same experimental conditions is shown for comparison.

exponential behavior even in the near-critical density region at low and high CBr₄ concentrations. The observed fluorescence lifetimes for 9CA are shown in Figure 5, and the results for anthracene, DPA, and perylene are similar. At a constant CBr₄ concentration, observed fluorescence lifetimes are clearly dependent on CO₂ reduced density. The lifetime of 9CA in the absence of CBr₄ decreases gradually with increasing CO₂ reduced density. In the presence of CBr₄, the observed fluorescence lifetime changes with CO₂ reduced density in a characteristic fashion. The lifetime first increases with increasing CO₂ reduced density and then levels off at reduced densities of ~ 1.4 and higher. Shown in Table 2 are fluorescence lifetime

TABLE 2: Fluorescence Lifetimes (τ_F , ns) at Different CBr_4 Concentrations and CO_2 Reduced Densities

[CBr_4], mM	CO_2 reduced density (35 °C)										
	0.8	0.9	1.0	1.1	1.2	1.3	1.4	1.5	1.6	1.7	1.8
	Anthracene										
0	7.93	7.87	7.81	7.75	7.69	7.63	7.58	7.52	7.47	7.41	7.36
2.40	4.80	4.86	4.94	5.07	5.15	5.20	5.24	5.29	5.36	5.47	5.64
3.00	3.64	3.81	3.98	4.14	4.30	4.46	4.61	4.76	4.91	5.05	5.19
6.16	2.25	2.44	2.62	2.79	2.96	3.12	3.27	3.42	3.56	3.70	3.82
	Perylene										
0	5.20	5.29	5.38	5.46	5.54	5.62	5.69	5.75	5.82	5.87	5.93
0.94	4.10	4.32	4.52	4.70	4.86	4.99	5.10	5.19	5.26	5.31	5.33
2.30	3.24	3.36	3.48	3.61	3.73	3.87	4.00	4.14	4.28	4.43	4.58
3.20	2.85	2.98	3.11	3.25	3.38	3.53	3.67	3.82	3.97	4.13	4.29
4.30	2.29	2.44	2.59	2.75	2.90	3.05	3.21	3.36	3.52	3.67	3.83
	9CA										
0	19.99	19.79	19.58	19.37	19.17	18.96	18.75	18.55	18.34	18.14	17.93
0.51	13.66	14.37	14.99	15.52	15.93	16.31	16.57	16.74	16.82	16.81	16.70
1.04	11.62	12.50	13.27	13.94	14.51	14.96	15.31	15.56	15.70	15.73	15.66
2.00	8.66	9.67	10.58	11.38	12.08	12.67	13.16	13.54	13.82	13.99	14.05
2.90	6.55	7.66	8.67	9.58	10.37	11.05	11.62	12.09	12.45	12.69	12.83
	DPA										
0	8.03	8.05	8.07	8.09	8.12	8.15	8.19	8.23	8.28	8.33	8.39
0.73	5.51	5.80	6.06	6.31	6.54	6.74	6.92	7.08	7.23	7.34	7.44
2.55	3.21	3.51	3.81	4.09	4.37	4.63	4.89	5.14	5.39	5.62	5.85
3.32	2.46	2.79	3.10	3.41	3.70	3.98	4.24	4.50	4.74	4.97	5.19

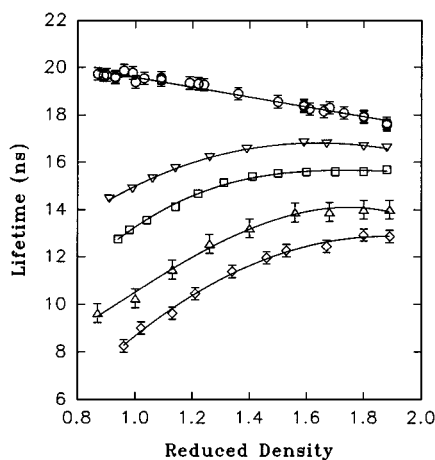


Figure 5. Observed fluorescence lifetimes of 9CA in supercritical CO_2 at 35 °C as a function of reduced density at CBr_4 concentrations of 0 (O), 5.14×10^{-4} (∇), 1.04×10^{-3} (□), 1.99×10^{-3} (Δ), and 2.9×10^{-3} M (◇). The empirical curves are for the interpolation of lifetime values at selected densities.

values at representative CO_2 reduced densities as a function of CBr_4 concentration, which were obtained from the experimental results through interpolation.

The lifetime data in Table 2 were analyzed in terms of the Stern–Volmer relationship (eq 1). For 9CA, Stern–Volmer plots at CO_2 reduced densities of 1.8, 1.6, 1.4, 1.2, and 1.0 are shown in Figure 6. The plots are reasonably linear, yielding Stern–Volmer quenching constants $k_q\tau_F^0$ of 135 M^{-1} at a high reduced density of 1.8 and 428 M^{-1} at a reduced density of 1.0. With the known fluorescence lifetimes of 9CA at the two reduced densities (Table 2), the fluorescence quenching rate constants k_q at the reduced densities of 1.8 and 1.0 are 7.9×10^9 and $2.2 \times 10^{10} \text{ M}^{-1} \text{ s}^{-1}$, respectively (Table 1).

The fluorescence lifetime quenching results of the anthracene– CBr_4 , DPA– CBr_4 , and perylene– CBr_4 systems in CO_2 (Table 2) were treated in the same fashion. Shown in Figure 7 are Stern–Volmer plots for anthracene– CBr_4 at CO_2 reduced densities of 1.8, 1.6, 1.4, 1.2, and 1.0. Linear least-squares regressions yield Stern–Volmer quenching constants ranging from 146 M^{-1} at a reduced density of 1.8 to 313 M^{-1}

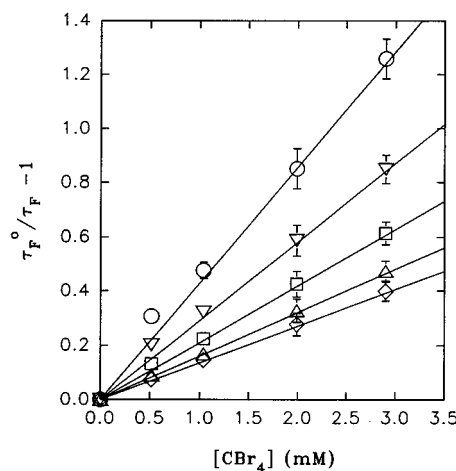


Figure 6. Stern–Volmer plots for the quenching of 9CA fluorescence lifetime by CBr_4 in supercritical CO_2 at 35 °C and reduced densities of 1.0 (O, 428 M^{-1}), 1.2 (∇, 290 M^{-1}), 1.4 (□, 209 M^{-1}), 1.6 (Δ, 160 M^{-1}), and 1.8 (◇, 135 M^{-1}). The lines are from linear least-squares regressions, with the slope values given in the corresponding parentheses.

at a reduced density of 1.0. With the known fluorescence lifetimes of anthracene in CO_2 (Table 2), the quenching rate constants k_q at CO_2 reduced densities of 1.8 and 1.0 are 2×10^{10} and $4 \times 10^{10} \text{ M}^{-1} \text{ s}^{-1}$, respectively (Table 1). The Stern–Volmer parameters for the fluorescence lifetime quenching results of DPA and perylene with CBr_4 in CO_2 at 35 °C are also summarized in Table 1 and Figure 8.

Discussion

The selection of arene– CBr_4 as model systems for studies in supercritical fluids is based on the expectation that their fluorescence quenching processes are simple bimolecular reactions.²⁸ Such expectations have been confirmed experimentally in the study of 9,10-bis(phenylethynyl)anthracene (BPEA)– CBr_4 ^{23a} and by the results reported here. In both room-temperature solution and supercritical CO_2 , excited singlet states of anthracene, 9CA, DPA, and perylene are quenched efficiently by CBr_4 without the formation of emissive excited-state complexes. There is also no evidence for any excitation

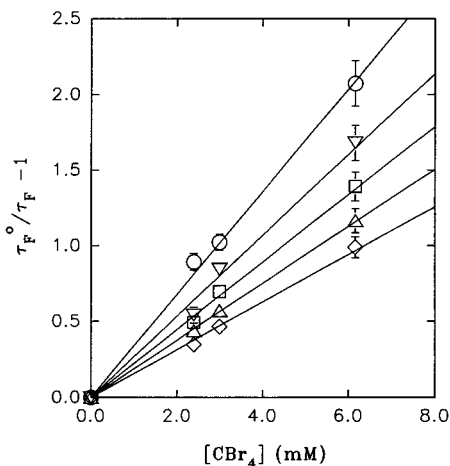


Figure 7. Stern–Volmer plots for the quenching of anthracene fluorescence lifetime by CBr₄ in supercritical CO₂ at 35 °C and reduced densities of 1.0 (○, 313 M⁻¹), 1.2 (▽, 255 M⁻¹), 1.4 (□, 211 M⁻¹), 1.6 (△, 175 M⁻¹), and 1.8 (◇, 146 M⁻¹). The lines are from linear least-squares regressions, with the slope values given in the corresponding parentheses.

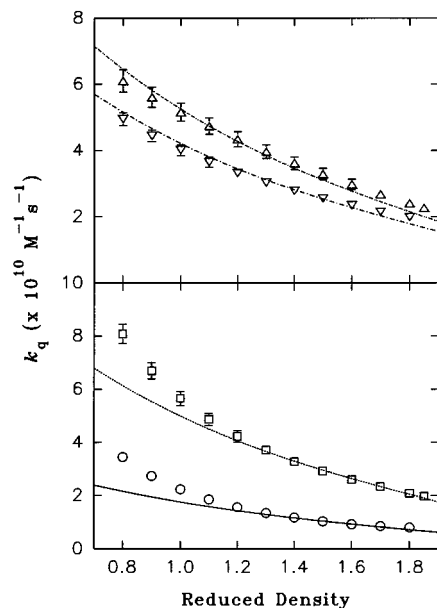


Figure 8. Observed quenching rate constants k_q at different reduced densities for anthracene–CBr₄ (top, ▽), perylene–CBr₄ (top, △), 9CA–CBr₄ (bottom, ○), and DPA–CBr₄ (bottom, □) in supercritical CO₂ at 35 °C. The lines represent the CO₂ density dependence of the Debye–Smoluchowski diffusion rate constants adjusted with the f factors (Table 1).

wavelength dependence in the fluorescence quenching and for any interference due to ground-state complexation and static quenching contributions.²⁸

As shown in Table 1, the quenching of arene excited states by CBr₄ is apparently at diffusion-controlled rates ($k_q \approx k_{diff}$). The diffusion rate constants k_{diff} may be estimated within the context of hydrodynamic theory in terms of the Smoluchowski equation

$$k_{diff} = 4 \times 10^{-3} \pi N(r_M + r_{CBr_4})(D_M + D_{CBr_4}) \quad (2)$$

where r_M and r_{CBr_4} are molecular radii of the arene molecule and the quencher CBr₄, respectively. Under a stick boundary condition, the diffusion coefficients $D_i = kT/6\pi\eta r_i$, where η is the shear viscosity of the solvent. A simplification by assuming $D_M = D_{CBr_4}$ results in the Debye–Smoluchowski equation,

$$k_{diff} = 8RT/3000\eta \quad (3)$$

For the quenching of anthracene fluorescence by CBr₄ in room-temperature hexane ($\eta = 0.31$ cP) and cyclohexane ($\eta = 0.96$ cP), the ratio of quenching rate constants predicted by eq 3 is 0.32. This is in reasonable agreement with the ratio of experimentally determined quenching rate constants for the two solvents (Table 1). However, the absolute values of k_{diff} from eq 3 are somewhat different from the experimentally determined quenching rate constants k_q obtained from the Stern–Volmer relationship. For example, the k_q value for anthracene–CBr₄ in cyclohexane obtained from the Stern–Volmer relationship is $1.25 \times 10^{10} \text{ M}^{-1} \text{ s}^{-1}$, which is larger than the k_{diff} value of $6.8 \times 10^9 \text{ M}^{-1} \text{ s}^{-1}$. Such discrepancies between the diffusion-controlled quenching rate constants k_q and k_{diff} are well-documented in the literature.²⁹ A factor f may be used to account for the difference.

$$k_q = f k_{diff} \quad (4)$$

The factor f is apparently system dependent even in a single solvent, 0.36 for 9CA–CBr₄ and 1.4 for anthracene–CBr₄ in room-temperature hexane. Similarly, the f values are different for different systems in supercritical CO₂ at 35 °C and a constant reduced density (Table 1).

The fluorescence quenching rate constants in supercritical CO₂ are also density dependent in a characteristic fashion. As shown in Figure 8, the observed k_q values increase systematically with decreasing CO₂ reduced density. The increases in k_q may be attributed to changes in CO₂ viscosity, which decreases by a factor of 2.5 from the reduced density of 1.8–1.0 at 35 °C. For anthracene–CBr₄, the dependence of observed k_q values on CO₂ reduced density may be described by using eq 4 with a constant f factor of 0.21, which can be obtained from the minimization of the residual $\sum(k_q - f k_{diff})^2$. The agreement between experimental and predicted results is good over the entire reduced density range (Figure 8). Also shown in Figure 8 is a similarly good agreement for perylene–CBr₄ with a constant f factor of 0.26.

For 9CA–CBr₄ and DPA–CBr₄, the observed quenching rate constants k_q depend on CO₂ reduced densities in a somewhat different fashion. At high CO₂ reduced densities (1.4 and higher), the results of anthracene–CBr₄ and perylene–CBr₄ may also be described by using eq 4 with constant f factors of 0.088 and 0.25, respectively. The agreement between the CO₂ density dependencies of k_q and k_{diff} in the high CO₂ density region is understandable because it is known that the solvent properties of high-density supercritical CO₂ are similar to those of normal liquids. However, at low CO₂ densities, increases in the observed quenching rate constants are much steeper than those predicted by the Debye–Smoluchowski equation (eq 3, Figure 8). Similar upward deviations have been observed in the fluorescence lifetime quenching of BPEA by CBr₄ in supercritical CO₂.^{23a}

For a more direct comparison, plots of k_q/f vs CO₂ reduced density for anthracene–CBr₄, 9CA–CBr₄, DPA–CBr₄, and perylene–CBr₄ are shown in Figure 9. Clearly, dependencies of the fluorescence quenching rate constants on CO₂ reduced density for anthracene–CBr₄ and perylene–CBr₄ are different from those for 9CA–CBr₄ and DPA–CBr₄. The quenching in anthracene–CBr₄ and perylene–CBr₄ is diffusion-controlled and is well described by the Debye–Smoluchowski equation. While the results for 9CA–CBr₄ and DPA–CBr₄ at high CO₂ densities are similar to those for anthracene–CBr₄ and perylene–CBr₄, there are significant upward deviations at low CO₂ densities (Figure 9), similar to that in the BPEA–CBr₄ system.^{23a}

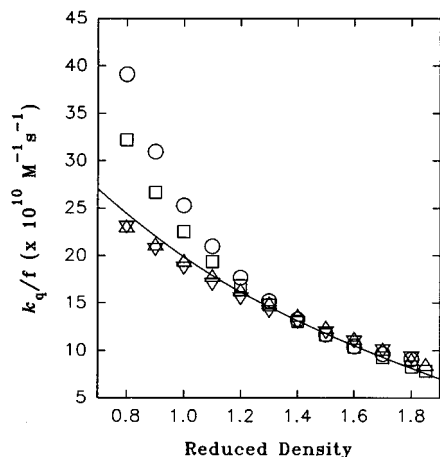


Figure 9. A plot of k_q/f vs CO_2 reduced density for anthracene- CBr_4 (∇), perylene- CBr_4 (Δ), 9CA- CBr_4 (\circ), and DPA- CBr_4 (\square). The line represents the CO_2 density dependence of the Debye-Smoluchowski diffusion rate constants.

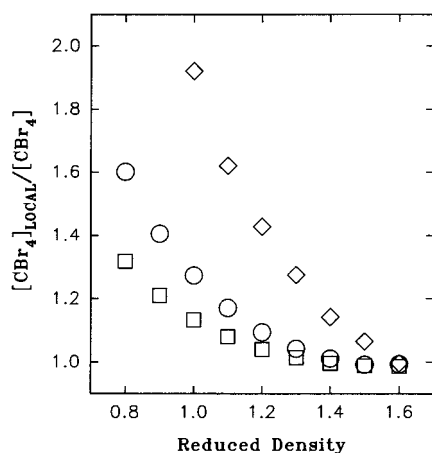


Figure 10. Plots of the ratio between local and bulk quencher concentrations vs reduced density for quenchings of 9CA (\circ), DPA (\square), and BPEA (\diamond)^{23a} fluorescence lifetimes by CBr_4 in supercritical CO_2 at 35 °C.

For BPEA- CBr_4 in supercritical CO_2 , the upward deviation in the density dependence of observed fluorescence quenching rate constants from the prediction of the hydrodynamic Smoluchowski equation has been attributed to enhanced bimolecular quenching due to higher local quencher concentrations in the near-critical density region.^{23a} A similar argument may be applied to the observed quenching rate constants for 9CA- CBr_4 and DPA- CBr_4 in CO_2 at near-critical densities. With the presence of effects due to local quencher concentration augmentation, the Stern-Volmer relationship may be rewritten as follows:^{23a}

$$\tau_F^\circ/\tau_F = 1 + k_q\tau_F^\circ[\text{CBr}_4]_{\text{LOCAL}} = 1 + k_q\tau_F^\circ\alpha[\text{CBr}_4] \quad (5)$$

where $\alpha = [\text{CBr}_4]_{\text{LOCAL}}/[\text{CBr}_4]$ becomes unity in the absence of local concentration effects. By assuming that k_q in eq 5 can be calculated from $f k_{\text{diff}}$ as in the CO_2 density dependence of fluorescence quenchings in anthracene- CBr_4 and perylene- CBr_4 systems (Figure 8), α values at different CO_2 reduced densities in the near-critical density region may be estimated using known bulk quencher concentrations $[\text{CBr}_4]$ and the calculated local quencher concentrations $[\text{CBr}_4]_{\text{LOCAL}}$. The results thus obtained are shown in Figure 10 along with the results for BPEA- CBr_4 reported previously.^{23a} While the α values clearly increase with decreasing CO_2 reduced density for all three systems, the magnitude of such increases is

apparently different from system to system. At a reduced density of 1.0, the α values for 9CA- CBr_4 and DPA- CBr_4 are 1.27 and 1.13, respectively, in comparison with an α value of 1.92 for BPEA- CBr_4 . Nevertheless, the strong system dependence is even more clearly demonstrated by the absence of any enhanced fluorescence quenching for the anthracene- CBr_4 and perylene- CBr_4 systems in supercritical CO_2 .

The mechanistic details behind the strong system dependence of enhanced fluorescence quenching at near-critical CO_2 densities are not clear. However, the results seem to suggest that properties of solute molecules may also play a critical role with respect to effects of local quencher concentration augmentation in bimolecular quenching reactions. With the same quencher CBr_4 , the five solute molecules that have been studied so far differ in molecular structures and in fluorescence quenching mechanisms. BPEA, 9CA, and DPA are structurally slightly different from anthracene and perylene because of the presence of substituent(s), though it is difficult to justify that such small structural differences would result in very different local quencher concentration augmentation effects. A more pronounced difference among these molecules is in their excited-state properties. For BPEA, 9CA, and DPA, fluorescence is essentially the only decay pathway with yields of unity.³⁰ While anthracene and perylene also have high fluorescence yields, intersystem crossing leading to the formation of excited triplet states is a significant competing decay pathway. Quenchings of anthracene and perylene fluorescence intensities and lifetimes by CBr_4 are at least partially due to heavy atom effects which result in more efficient intersystem crossing processes. Such an assessment is supported by the observation of photochemical bleaching of anthracene and perylene in the presence of CBr_4 , which is likely due to enhanced photochemical reactions through their excited triplet states. Quenchings of the excited singlet states of BPEA, 9CA, and DPA by CBr_4 are probably dominated by electron-transfer processes.²⁸ Although there is no evidence suggesting that the mechanistic difference in fluorescence quenching processes is responsible for the system dependence in local quencher concentration effects, it remains a possible explanation for further experimental and theoretical investigations.

The applicability of the hydrodynamic equation to the diffusion-controlled fluorescence quenching processes in supercritical CO_2 at different densities should also be considered. It is a possibility that the factor f might be CO_2 density dependent, though it would be difficult to understand why such a dependence becomes evident only for fluorescence quenchings in the BPEA- CBr_4 , 9CA- CBr_4 , and DPA- CBr_4 systems. In addition, there are no reports in the literature suggesting that diffusional processes in supercritical fluids can be more efficient than those predicted in terms of the hydrodynamic equation. The solute-solvent clustering or local solvent density augmentation in supercritical fluids apparently has little effect on diffusion-controlled bimolecular reactions such as the photodimerization of anthracene.³¹ In fact, it would be reasonable to expect that the solute-solvent clustering or local solvent density augmentation at near-critical densities should hinder bimolecular diffusional processes rather than making the processes more efficient as is required to explain the fluorescence quenching results of the BPEA- CBr_4 , 9CA- CBr_4 , and DPA- CBr_4 systems. In such a context, it may be concluded that the significant discrepancies between observed quenching rate constants and hydrodynamic diffusion rate constants are unlikely due to the breakdown of the hydrodynamic equation in supercritical CO_2 .

The results presented here clearly demonstrate, for the first

time, that effects of local solute concentration augmentation in supercritical CO₂ at near-critical densities are in fact system dependent. Further efforts are necessary in order to address the mechanistic details.

Acknowledgment. We thank J. E. Riggs for experimental assistance. Y.-P.S. acknowledges financial support from the donors of the Petroleum Research Fund, administered by the American Chemical Society, and in part from the National Science Foundation (CHE-9320558). J.R.G. acknowledges Dr. Julian Tishkoff and the Air Force Office of Scientific Research (AFOSR) for continuing support of supercritical fluids research. C.E.B. thanks AFOSR for support through the Summer Graduate Research Program.

References and Notes

- (1) (a) Penninger, J. M. L.; Radosz, M.; McHugh, M. A.; Krukoni, V. J., Eds. *Supercritical Fluid Technology*; Elsevier: Amsterdam, 1985. (b) McHugh, M. A.; Krukoni, V. J. *Supercritical Fluid Extraction, Principles and Practice*; Butterworth: Stoneham, 1986.
- (2) Shaw, R. W.; Brill, T. B.; Clifford, A. A.; Eckert, C. A.; Franck, E. U. *Chem. Eng. News* **1991**, Dec 23, 26.
- (3) (a) Savage, P. E.; Gopalan, S.; Mizan, T. I.; Martino, C. J.; Brock, E. E. *AIChE J.* **1995**, *41*, 1723. (b) Clifford, T.; Bartle, K. *Chem. Ind.* **1996**, 449.
- (4) Kim, S.; Johnston, K. P. *Ind. Eng. Chem. Res.* **1987**, *26*, 1206.
- (5) Bennett, G. R.; Johnston, K. P. *J. Phys. Chem.* **1994**, *98*, 441.
- (6) Brennecke, J. F.; Tomasko, D. L.; Peshkin, J.; Eckert, C. A. *Ind. Eng. Chem. Res.* **1990**, *29*, 1682.
- (7) Eckert, C. A.; Knutson, B. L. *Fluid Phase Equilib.* **1993**, *83*, 93.
- (8) (a) Yonker, C. R.; Frye, S. L.; Kalkwarf, D. R.; Smith, R. D. *J. Phys. Chem.* **1986**, *90*, 3022. (b) Smith, R. D.; Frye, S. L.; Yonker, C. R.; Gale, R. W. *J. Phys. Chem.* **1987**, *91*, 3059. (c) Yonker, C. R.; Smith, R. D. *J. Phys. Chem.* **1988**, *92*, 235.
- (9) (a) Betts, T. A.; Bright, F. V. *Appl. Spectrosc.* **1990**, *44*, 1196, 1203. (b) Betts, T. A.; Zagrobelny, J.; Bright, F. V. *J. Supercrit. Fluids* **1992**, *5*, 48.
- (10) (a) Kajimoto, O.; Futakami, M.; Kobayashi, T.; Yamasaki, K. *J. Phys. Chem.* **1988**, *92*, 1347. (b) Morita, A.; Kajimoto, O. *J. Phys. Chem.* **1990**, *94*, 6420.
- (11) Sun, Y.-P.; Fox, M. A.; Johnston, K. P. *J. Am. Chem. Soc.* **1992**, *114*, 1187.
- (12) (a) Randolph, T. W.; Carlier, C. *J. Phys. Chem.* **1992**, *96*, 5146. (b) Carlier, C.; Randolph, T. W. *AIChE J.* **1993**, *39*, 876.
- (13) Howdle, S.; Bagratashvili, V. N. *Chem. Phys. Lett.* **1993**, *214*, 215.
- (14) (a) Sun, Y.-P.; Bunker, C. E.; Hamilton, N. B. *Chem. Phys. Lett.* **1993**, *210*, 111. (b) Sun, Y.-P.; Bunker, C. E. *Ber. Bunsen-Ges. Phys. Chem.* **1995**, *99*, 976.
- (15) O'Brien, J. A.; Randolph, T. W.; Carlier, C.; Shankar, G. *AIChE J.* **1993**, *39*, 1061.
- (16) Worrall, D. R.; Wilkinson, F. J. *Chem. Soc., Faraday Trans.* **1996**, *92*, 1467.
- (17) Kim, S.; Johnston, K. P. *AIChE J.* **1987**, *33*, 1603.
- (18) Combes, J. R.; Johnston, K. P.; O'Shea, K. E.; Fox, M. A. In *Supercritical Fluid Science and Technology*; Johnston, K. P., Penninger, J. M. L., Eds.; American Chemical Society: Washington, DC, 1989; p 31.
- (19) Kazarian, S. G.; Gupta, R. B.; Clarke, M. J.; Johnston, K. P.; Poliakoff, M. *J. Am. Chem. Soc.* **1993**, *115*, 11099.
- (20) Gupta, R. B.; Combes, J. R.; Johnston, K. P. *J. Phys. Chem.* **1993**, *97*, 707.
- (21) (a) Zagrobelny, J.; Betts, T. A.; Bright, F. V. *J. Am. Chem. Soc.* **1992**, *114*, 5249. (b) Rice, J. K.; Niemeyer, E. D.; Dunbar, R. A.; Bright, F. V. *J. Am. Chem. Soc.* **1995**, *117*, 5832.
- (22) (a) Roberts, C. B.; Zhang, J.; Brennecke, J. F.; Chateaufeuf, J. E. *J. Phys. Chem.* **1993**, *97*, 5618. (b) Roberts, C. B.; Zhang, J.; Chateaufeuf, J. E.; Brennecke, J. F. *J. Am. Chem. Soc.* **1993**, *115*, 9576.
- (23) (a) Bunker, C. E.; Sun, Y.-P. *J. Am. Chem. Soc.* **1995**, *117*, 10865. (b) Sun, Y.-P.; Bunker, C. B. *J. Phys. Chem.* **1995**, *99*, 13778.
- (24) (a) Kurnik, R. T.; Reid, R. C. *Fluid Phase Equilib.* **1982**, *8*, 93. (b) Kwiatkowski, J.; Lisicki, Z.; Majewski, W. *Ber. Bunsen-Ges. Phys. Chem.* **1984**, *88*, 865.
- (25) O'Connor, D. V.; Phillips, D. *Time-Correlated Single Photon Counting*; Academic Press: New York, 1984.
- (26) Stephan, K.; Lucas, K. *Viscosity of Dense Fluids*; Plenum Press: New York, 1979.
- (27) (a) Jossi, J. A.; Stiel, L. I.; Thodos, G. *AIChE J.* **1962**, *8*, 59. (b) Reid, R. C.; Prausnitz, J. M.; Poling, B. E. *The Properties of Gases and Liquids*; McGraw-Hill: New York, 1987.
- (28) (a) Birks, J. B. *Photophysics of Aromatic Molecules*; Wiley-Interscience: London, 1970. (b) Birks, J. B. In *Organic Molecular Photophysics*; Birks, J. B., Ed.; Wiley: London, 1975; Vol. 2, Chapter 9.
- (29) Saltiel, J.; Atwater, B. W. *Adv. Photochem.* **1988**, *14*, 1.
- (30) (a) Lampert, R. A.; Meech, S. R.; Metcalfe, J.; Phillips, D.; Schaap, A. P. *Chem. Phys. Lett.* **1983**, *94*, 137. (b) Hirayama, S.; Iuchi, Y.; Tanaka, F.; Shobatake, K. *Chem. Phys.* **1990**, *144*, 401.
- (31) Bunker, C. E.; Rollins, H. W.; Gord, J. R.; Sun, Y.-P. *J. Org. Chem.* **1997**, *62*, 7324.